LOCKIN THERMOGRAPHY METHODS FOR THE NDT OF CFRP AIRCRAFT COMPONENTS

Th. Zweschper[1], A. Dillenz[1], G. Riegert[1], D. Scherling[2] and G. Busse[1]
[1]University of Stuttgart – Institute of Polymer Testing and Polymer Science (IKP), Department of Non-destructive Testing, Pfaffenwaldring 32, D-70569 Stuttgart, Germany (zweschper@ikp.uni-stuttgart.de)
[2]Airbus Germany GmbH, Huenefeldstrasse 1-5, D-28199 Bremen, Germany

Abstract

Optically excited lockin thermography (OLT) is based on propagation and reflection of thermal waves which are launched from the surface into the inspected component by absorption of modulated radiation. Phase angle images obtained by superposition of the initial thermal wave and its internal reflection display hidden thermal structures down to a certain depth below the surface. Defects are found by comparing the observed features with expected features provided by theory or by an intact reference sample.

Elastic waves sent into the component propagate inside the sample until they are converted into heat. A defect causes locally enhanced losses and consequently selective heating up. Therefore modulation of the elastic wave amplitude results in periodical heat generation so that the defect is turned into a local thermal wave transmitter. Its emission is detected via the temperature modulation at the surface which is analysed by lockin thermography tuned to the frequency of amplitude modulation. The amplitude image displays the efficiency of mechanical losses, so it shows the imaginary part of local elastic properties.

Introduction

Reliable inspection techniques are required for the maintenance of safety relevant structures (e.g. aerospace equipment and vehicles) where one needs to detect defect areas early enough to prevent catastrophic failure. As many structures consist of carbon fibre reinforced plastics (CFRP), the rapid and remote identification of delaminations, impact damages, ruptures, and cracks is a topic of major concern. Therefore a method is required that is applicable during inspection procedures to monitor the integrity of such structures.

External excitation :Optical Lockin Thermography (OLT)

Thermal waves (1) have been used very early for remote monitoring of thermal features, e.g. cracks, delaminations (2), and other kinds of boundaries. After the advantage of signal phase had been discovered (3-5), phase angle imaging using photothermal techniques (6) became a powerful tool for imaging of hidden structures due to the enhanced depth range and its independence on optical (7) or infrared surface patterns.

As the thermal diffusion length is the important parameter for depth range (8), it turned out very soon that imaging of features deep underneath the surface requires very low modulation frequencies and a correspondingly long time to obtain a photothermal image. Unfortunately many industrial questions are related to samples with defects at about a millimeter depth. An image obtained pixel after pixel at a modulation frequency in the 1 Hz range could easily require several hours.

One approach allowing for a reduction of inspection time is lockin thermography where the low frequency thermal wave is generated simultaneously on the whole surface of the inspected component and monitored everywhere several times per modulation cycle in order to obtain an image of amplitude and phase of temperature modulation (9-12). In this case the inspection time is given by a few modulation cycles. As one can image square meters of airplanes within a few minutes (13), one has a powerful method for fast inspection of safety relevant structures with a depth range of several millimetres in CFRP.

Figure 1 shows the principle and the set-up of optical excited lockin thermography. Absorption of intensity modulated radiation generates on the whole surface a thermal wave. It propagates into the interior where it is reflected at boundaries and defects so that it moves back to the surface where it is superposed to the initial wave. This way a defect is revealed by the local change of phase angle.

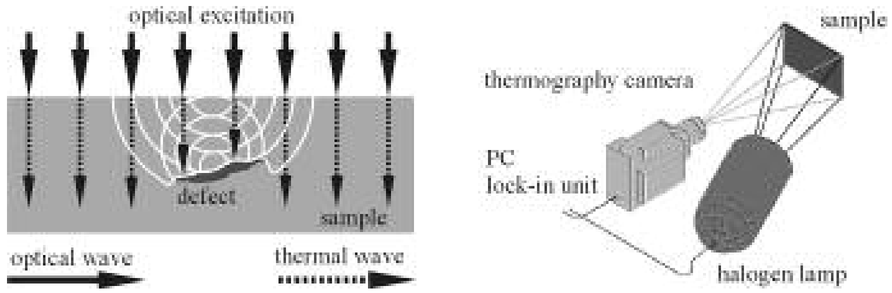

Figure 1. Principle and set-up of lockin thermography with optical excitation.

Therefore both defects and intact structures are imaged at the same time. Defects can be revealed only by comparing the observed features with expected patterns provided by theory, by reference samples, or by design drawings. Even for an experienced inspector it is difficult to distinguish defect areas from these thermal features.

Internal excitation : Ultrasound Lockin Thermography (ULT)

Further investigations aimed at a method where a defect responds selectively so that the image would display only the defect and not the confusing background of the intact structure. Defects differ from their surroundings by their mechanical weakness. They may cause stress concentrations, and under periodical load there may be hysteresis effects or friction in cracks and delaminations. As defects may be areas where mechanical damping is enhanced, the ultrasound is converted into heat mainly in defects (14, 15). Modulation of the elastic wave amplitude results in periodical heat generation so that the defect is turned into a local thermal wave transmitter (Figure 2). Its emission is detected via the temperature modulation at the surface which is analysed by lockin thermography tuned to the frequency of amplitude modulation (16). The ultrasonic transducer is attached at a fixed spot from where the acoustic waves are launched into the whole volume where they are reflected several times until they disappear preferably in a defect and generate heat. These high frequencies are very efficient in heating since many hysteresis cycles are performed per second.

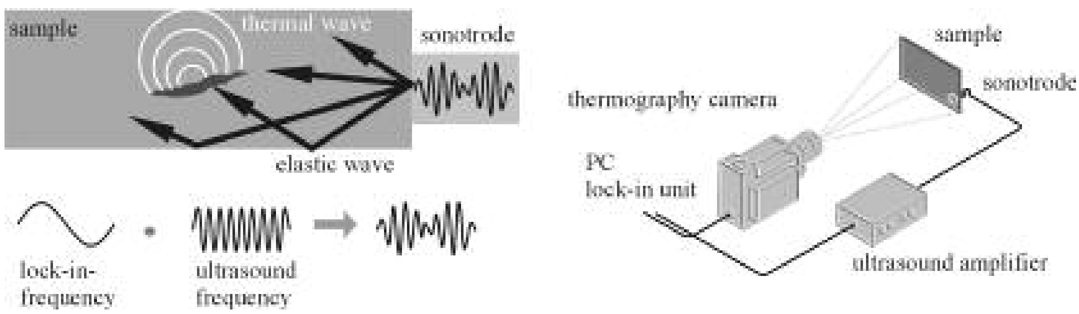

Figure 2. Principle and set-up of lockin thermography with ultrasonic excitation.

Internal excitation :Ultrasound Burst Phase Thermography (UBP)

Another established method is the use of short sonic bursts for sample excitation (17) (Figure 3). The spectral components of that signal and the following cooling down period provide information about defects in almost the same way as Lockin technique but with reduced measuring duration. As the characteristic defect signal is contained in a limited spectral range while the noise typically is distributed over the whole spectrum, one can reduce noise as well. That kind of evaluation technique using Fourier or Wavelet transformations is also applicable to flash light excited thermography (18-20). The signal to noise ratio of ULT and UBP images (and hence defect detectability) is significantly better than just one temperature snapshot image in a sequence (21, 22).

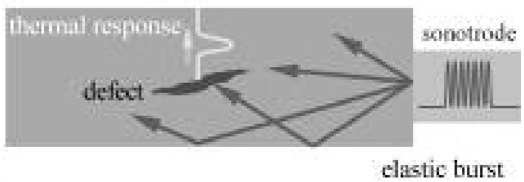

Figure 3. Principle of ultrasound burst thermography.

The following example confirms that high frequencies probe only near-surface areas while low frequencies with their larger depth range provide information about defects deeper inside the component. Thus depth resolved mapping of defects can be performed with only one measurement.

For this demonstration we manufactured a sample which had four delaminations in various depths between 0.2 mm and 2.2 mm. After an ultrasonic burst of 100 ms duration had been applied the resulting temperature sequence was evaluated at different frequencies. In the phase image at 3 Hz (Figure 4a) only the defect next to the surface causes a change in the phase angle. At 1 Hz (Figure 4b) already three delaminations in depths from 0.2 mm to 1.5 mm become visible. At 0.5 Hz (Figure 4c) all defects appear. At an even lower frequency (0.1 Hz, see Figure 4d) the image contrast is reduced due to lateral diffusion effects.

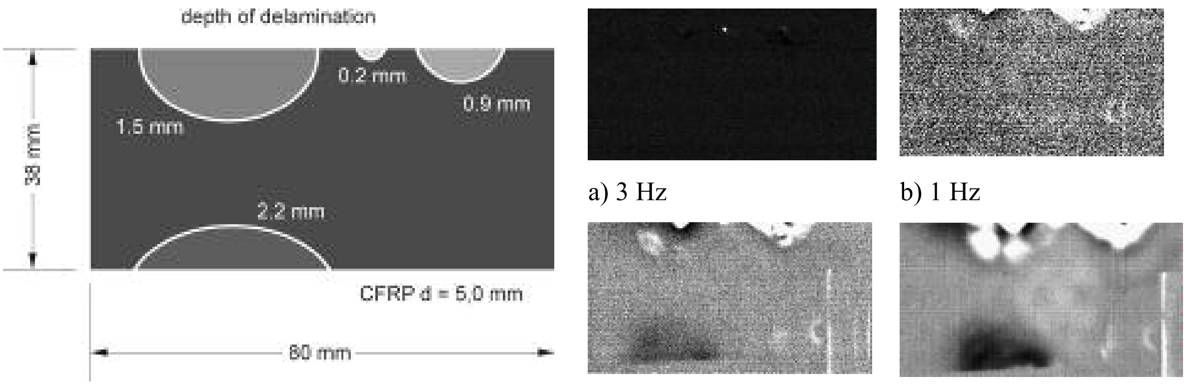

a) 3 Hz b) 1 Hz

c) 0,5 Hz d) 0,1 Hz

Figure 4. UBP images of a CFRP sample with delaminations in different depths. Excitation: 1 kW, ultrasonic frequency 20 kHz, burst duration: 100 ms.

Due to the signifance of non-destructive inspection for safety-relevant structures we applied these techniques (OLT, ULT, and UBP) to various CFRP components of aircraft. The results using this defect-selective technique will be described below.

Results

Ruptures, delaminations, and cracks in CFRP stringer structures

Stringers are used if stiffness needs to be enhanced along a certain direction. Stringer disbond caused e.g. by excessive loading therefore results in a loss of structural stiffness. Therefore one is highly interested to detect such defects early enough to prevent failure.

Ruptures of stringers in aerospace components are a serious problem because this kind of damage is almost invisible from the outer surface of an aircraft for most non-destructive testing methods, since stringers are hidden behind a panel. The access from inside the aircraft is difficult and time consuming.

The CFRP structure to be inspected had ruptures in its stringers as shown in Figure 5a schematically. The damage was covered by a CFRP skin with a thickness of more than 6 mm. While stringer delaminations can be detected with Optical Lockin Thermography (13), the depth range of optically generated thermal waves is not sufficient to reveal hidden stringer ruptures (Figure 5b). Ultrasound Lockin Thermography (Figure 5c and 5d) and Ultrasound Burst Phase image (Figure 5e) can reveal the rupture in the left stringer clearly. The damage in the right stringer is too far from the surface (30 mm), therefore it remains undetected even with sonic excitation.

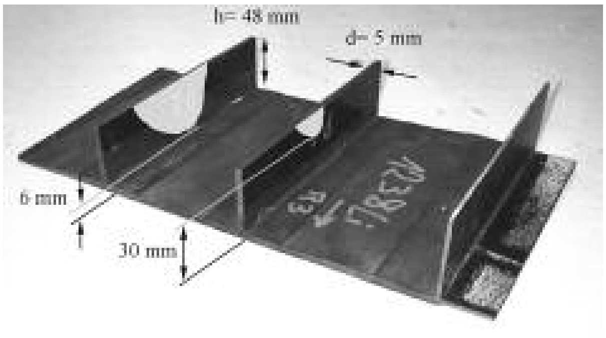

a) CFRP stringer structure
thickness of skin: 6 mm.
Laminated stringer (thickness 5 mm, height 48 mm).
Ruptures are marked white.

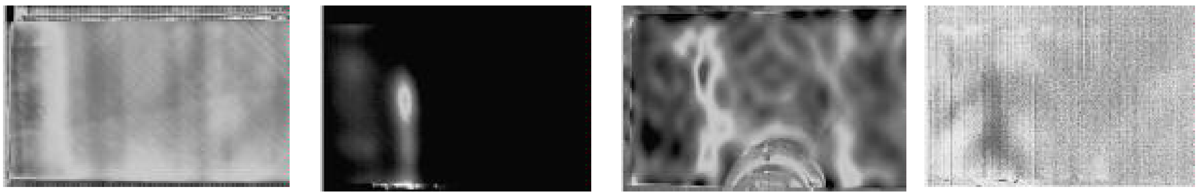

b) Optical Lockin Thermography Phase image at 0.01 Hz, 200 seconds acquisition time

c) Ultrasound Lockin Amplitude image at 0.01 Hz, 400 W, and 100 seconds acquisition time

d) Ultrasound Lockin Phase image at 0.01 Hz, 400 W, and 100 seconds acquisition time

e) Ultrasound Burst Phase image at 0,0485 Hz, burst length 5s, 400 W

Figure 5. Comparison of different phase images of ruptures in a aerospace component

Another example is the flap shown in Figure 6 where the results of OLT and ULT are compared. While OLT displays the whole structure where the small effect of the defect readily escapes attention, a small white spot in the ULT image indicates a crack and a delamination in the stringer underneath the intact CFRP-skin.

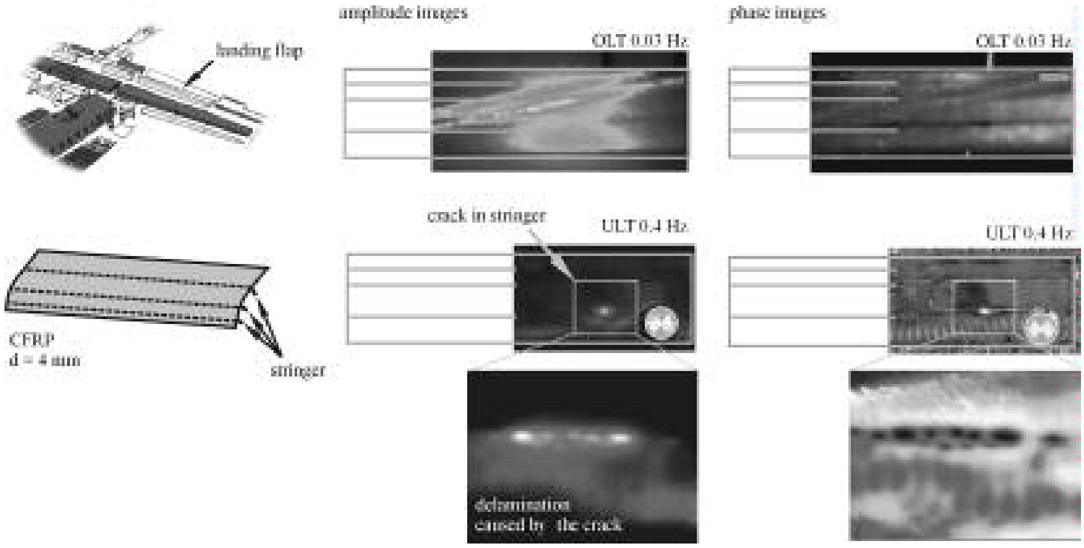

Figure 6. Comparison of OLT and ULT images of a delamination caused by a crack

Another example is the component investigated previously (23). The photograph of the rear surface displays the structure that needs to be inspected with access only from the flat front surface. It is composed of a CFRP skin and T-shaped stringers bonded to it while the lighter rectangular areas are glass fiber reinforced polymer (GFRP) wedges attached to the structure to perform tests under load. With OLT performed on the front surface the intact structure (including the GFRP area) is revealed where the disbond appears as an interruption of the straight lines which indicate the bonded stringers. The ULT phase image shows only the area where the disbond starts since only there the components can rub against each other in the ultrasound field. Surprisingly, there is an additional small spot which is not due to disbond but rather to a crack in the perfectly bonded stringer so that the heat modulation generated by friction can propagate as a thermal wave across the bond into the front of the skin over a cm-distance.

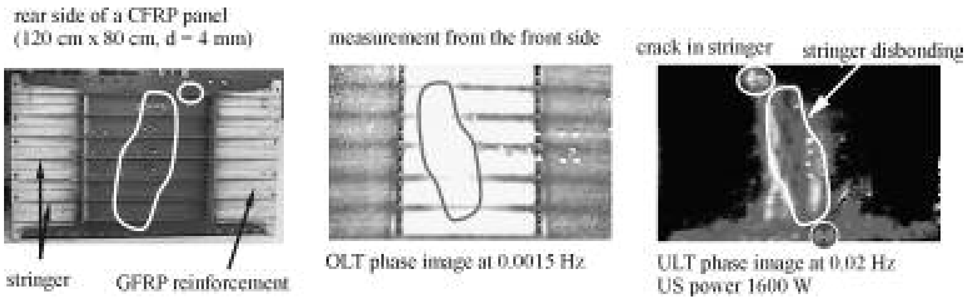

Figure 7. Stringer disbonding and cracks in an aircraft panel. OLT (left) and ULT (right).

Damage detection using small piezo-ceramic actuators

From previous investigations it is known that soft materials could be damaged by injecting elastic waves with high energy (24). An alternative approach is the use of many small distributed piezo-ceramic actuators to generate an elastic wave field in the inspected component. This results in a reduction of mechanical and thermal load. Here we examined a thin carbon fiber plate with seven impact damages. Three piezo-ceramic actuators were bonded to the sample to generate a wave field at a frequency of 8 kHz with 200 W for 1 second. Some milliseconds after the excitation burst, the best thermal contrast for defect detection is achieved (Figure 8 a). However, there is only a small change in temperature at the damaged regions of the sample. The amplitude image calculated with a Fourier transform at 0.24 Hz is an improvement in terms of signal to noise ratio (Figure 8b). The defects are displayed with better contrast, but friction between sample and actuators causes thermal fringes around the actuators. This effect is reduced in the phase image (Figure 8c), where inhomogenities of temperature variations are eliminated.

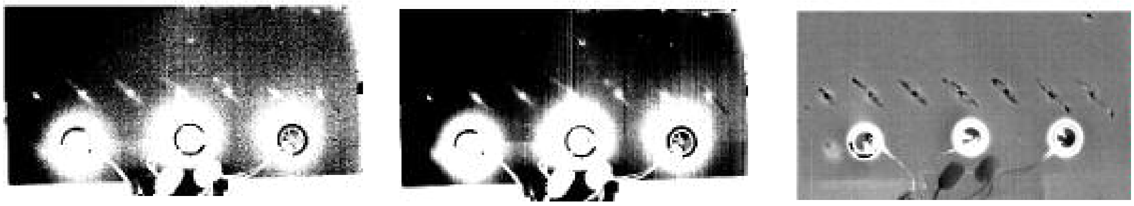

a) Temperature image one second after sound injection.

b) UBP: amplitude image at 0.24 Hz

c) UBP: phase image at 0.24 Hz

Figure 8. UBP: amplitude and phase image of seven impacts in CFRP (d = 2 mm)

Growing dimensions of new aircraft require rigid and lightweight structures. Fibre composites such as CFRP are increasingly being used since they satisfy these demands. The wall thickness of these structures is growing also, causing problems with many established non-destructive testing methods.

An example is the examination of a 9 mm thick CFRP plate with OLT. Six areas of heat damage are at the rear side of the sample (Figure 9). Limited depth range of optically excited thermal waves prevents a successful application of this remote technique. The damages remain undetected. The use of sonic excitation improves the situation. With an excitation power of 0.5 kW and acquisition time of 100 seconds, both heat damages are revealed. Using the burst phase technique, a reduction of acquisition time is possible. The result looks similar to the Lockin measurement, the measurement time, however, is reduced from 100 seconds to only 16 seconds.

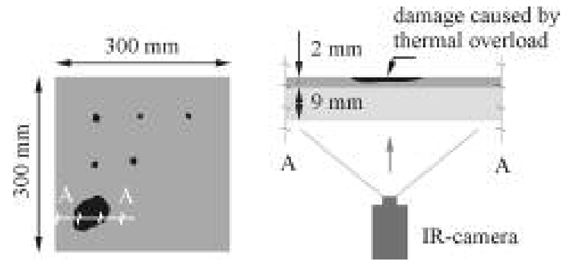

before reinforcement d=2 mm		after reinforcement d=9 mm		
OLT	ULT	OLT	ULT	UBP
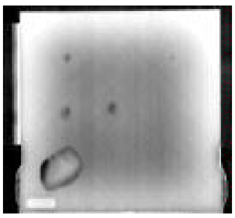	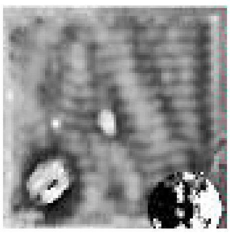	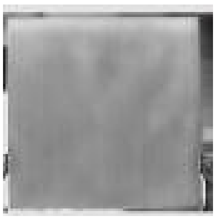	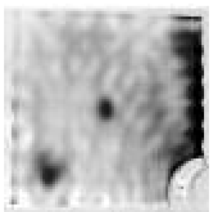	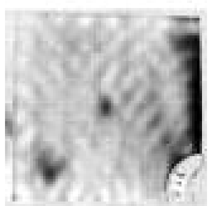
0,01 Hz phase image	0,01 Hz phase image 500 W	0,01 Hz phase image	0,01 Hz phase image, 500W	Burst length 500 ms, 1kW, phase image at 0,06 Hz

Figure 9. Comparison of Ultrasound Burst Phase evaluation and Lockin technique

Conclusion

Phase Thermography (Lock-in or Burst) has some advantages as compared to conventional pulse thermography: sensitivity variations within the detector array as well as optical sample characteristics are suppressed. Furthermore the signal to noise ratio is improved significantly. Compared to OLT, using the ULT / UBP methods in CFRP defects can be detected up to a depth of 12 mm. Using UBP the probability of defect identification is thus improved at a reduced measuring time. The measurements presented in this paper show that even larger components can be examined with this technique.

However, the high excitation power contained in short pulses or bursts could possibly cause damage of the inspected structure. Standing waves can occur if the frequency applied to the sample is at a mechanical resonance. Due to hysteretic losses in the elongation maximum, these standing elastic waves can appear as temperature patterns. which can cause misinterpretations. To eliminate standing wave patterns and to reduce the high excitation power the application of small piezo-ceramic actuators was investigated. Good results where found for relatively small samples. However, the excitation efficiency must be improved to make this technique applicable to non-destructive testing of large stru tures.

References

(1) Fourier J.: Théorie du mouvement de la chaleur dans les corps solides, 1re Partie. In: Mémoires de l'Académie des Sciences 4 (1824) pp.185-555.

(2) Wong Y. H.; Thomas R. L.; Pouch J. J.: Subsurface structures of solids by scanning photoacoustic microscopy. In: Appl. Phys. Lett. 35 5 (1979) pp. 368-369.

(3) Busse G.: Optoacoustic phase angle measurement for probing a metal. In: Appl. Phys. Lett. Vol. 35 (1979) pp. 759-760.

(4) Thomas R. L.; Pouch J. J.; Wong Y. H.; Favro L. D.; Kuo P. K.; Rosencwaig A.: Subsurface flaw detection in metals by photoacoustic microscopy. In: J. Appl. Phys. Vol. 51 (1980): pp. 1152-1156.

(5) Lehto A.; Jaarinen J.; Tiusanen T.; Jokinen M.; Luukkala M.: Amplitude and phase in thermal wave imaging. In: Electr. Lett. Vol. 17 (1981): pp. 364-365.

(6) Nordal, P.-E.; Kanstad S.O.: Photothermal radiometry. In: Physica Scripta Vol. 20 (1979): pp. 659-662.

(7) Rosencwaig A.; Busse G.: High resolution photoacoustic thermal wave microscopy. In: Appl. Phys. Lett. Vol. 36 (1980): pp. 725-727.

(8) Rosencwaig A.: Photoacoustic microscopy. In: American Lab. 11 (1979) pp. 39-49.

(9) Carlomagno G. M.; Berardi P. G.: Unsteady thermotopography in non-destructive testing. In: Proc. 3rd Biannual Exchange, St. Louis/USA, 24.-26. August 1976, pp. 33-39.

(10) Beaudoin J. L.; Merienne E.; Danjoux R.; Egee M.: Numerical system for infrared scanners and application to the subsurface control of materials by photothermal radiometry. In: Infrared Technology and Applications, SPIE Vol. 590 (1985) p. 287.

(11) Kuo, P.K.; Feng Z. J.; Ahmed T.; Favro L. D.; Thomas R. L.; Hartikainen J.: Parallel thermal wave imaging using a vector lock-in video technique. In: Photoacoustic and Photothermal Phenomena, ed. P. Hess and J. Pelzl. Heidelberg: Springer-Verlag. (1987) pp. 415-418.

(12) Busse, G., Wu D. and Karpen W.: Thermal wave imaging with phase sensitive modulated thermography. In: J. Appl. Phys. Vol. 71 (1992): pp. 3962-3965.

(13) Wu, D.; Salerno A.; Malter U.; Aoki R.; Kochendörfer R.; Kächele P. K.; Woithe K.; Pfister K.; Busse G.: Inspection of aircraft structural components using lockin-thermography. In: Quantitative infrared thermography, QIRT 96, Stuttgart, ed. D. Balageas, G. Busse, and G. M. Carlomagno. Pisa: Edizione ETS (1997): pp. 251-256. ISBN 88 - 467 - 0089 – 9

(14) Mignogna R. B.; Green R. E., Jr.; Duke; Henneke E. G.; Reifsnider K.L.: Thermographic investigations of high-power ultrasonic heating in materials. In: Ultrasonics 7 (1981) pp. 159-163.

(15) Stärk F.: Temperature measurements on cyclically loaded materials. In: Werkstofftechnik 13, Verlag Chemie GmbH, Weinheim (1982) pp. 333-338.

(16) Rantala J.; Wu D.; Busse G.: Amplitude Modulated Lock-In Vibrothermography for NDE of Polymers and Composites. In: Research in Nondestructive Evaluation, Vol. 7 (1996) pp. 215-218.

(17) Patent DE 100 59 854.4

(18) Maldague, X.; Marinetti, S.; Pulse Phase Infrared Thermography, J. Appl. Phys, 79 [5]: 2694-2698, 1 March 1996.

(19) F. Galmiche, S. Vallerand, X. Maldague, Pulsed Phase Thermography with the Wavelet Transform, Review of Progress in Quantitative NDE, D.O. Thompson et D.E. Chimenti eds, Am. Institute of Physics, 19A: S. 609-615, (Montréal Juli 1999), 2000.

(20) Maldague, X.; Marinetti, S.; Busse, G.; Couturier, J.-P.: Possible applications of pulse phase thermography. Progress in Natural Science. Supplment to Vol. 6, December 1996, S. 80-82

(21) L. D. Favro, Xiaoyan Han, Zhong Ouyang, Gang Sun, Hua Sui, and R. L.Thomas, Infrared imaging of defects heated by a sonic pulse, Rev. Sci. Inst. 71, 6, 2000, S. 2418-2421.

(22) R. L. Thomas, L.D. Favro, P. K. Kuo, T. Ahmed, Xiaoyan Han, Li Wang, Xun Wang and S.M. Shepard, Pulse-Echo Thermal-Wave Imaging for Non-Destructive Evaluation, Proc. 15th International Congress on Acoustics, Trondheim, Norway, June 26-30, 1995, S. 433-436.

(23) Salerno, A.; Dillenz, A.; Wu, D.; Rantala, J.; Busse; G.: Progress in ultrasonic lockin thermography. Quantitative infrared thermography, QIRT 98. Akademickie Centrum Graficzno-Marketingowe Lodart S.A., Lodz 1998, S. 154-160. ISBN 83-87202-88-6

(24) Dillenz, D.; Zweschper, Th.; Busse, G.: Progress in ultrasound phase angle thermography, Thermosense 2001, Orlando, USA.